Journal of Applied Polymer Science

Flexible polyurethane foams modified with biobased polyols: Synthesis and physical-chemical characterization

G. D. Soto, N. E. Marcovich, M. A. Mosiewicki
Instituto de Investigaciones en Ciencia y Tecnología de Materiales (INTEMA), Universidad Nacional de Mar del Plata–Consejo Nacional de Investigaciones Científicas y Técnicas (CONICET), Av. J. B. Justo 4302, 7600, Mar del Plata, Argentina
Correspondence to: M. A. Mosiewicki (E-mail: mirna@fi.mdp.edu.ar)

ABSTRACT: A series of flexible polyurethane foams with different polyol compositions were synthesized through the replacement of a portion of the petroleum-based polyether polyol with biobased polyols, namely, glycerol (GLY) and hydroxylated methyl esters (HMETO). HMETO was synthesized by the alkaline transesterification of tung oil (TO; obtaining GLY as a byproduct) and the subsequent hydroxylation of the obtained methyl esters with performic acid generated *in situ*. FTIR spectroscopy, ^{1}H-NMR, and different analytical procedures indicated that the hydroxyl content increased significantly and the molecular weight decreased with respect to those of the TO after the two reaction steps. The characterization of the obtained foams, achieved through the measurement of the characteristic reaction times, thermal and dynamic mechanical analysis, scanning electronic microscopy, and density measurements, is reported and discussed. The most important changes in the modified foams were found with the addition of GLY to the formulation; this led to an increased foam density and storage rubbery modulus, which were associated with a higher crosslinking density because of the decrease in the chain length between crosslinking points. © 2016 Wiley Periodicals, Inc. J. Appl. Polym. Sci. **2016**, *133*, 43833.

KEYWORDS: biopolymers and renewable polymers; polyurethanes; properties and characterization

Received 24 November 2015; accepted 18 April 2016
DOI: 10.1002/app.43833

INTRODUCTION

Flexible polyurethane foams (FPs) belong to a well-known class of polymeric materials that are widely used in daily applications such as furnishings, transportation, packaging cushioning, and automotive seating.[1–3] At present, FPs are also gaining great interest in novel areas such as biomedicine, intelligent materials, and nanocomposites.[4] These foams offer degrees of comfort, protection, and utility not matched by any other single cushioning material. Through the appropriate selection of the reactants and manufacturing process, polyurethane (PU) foams can be tailored to satisfy a wide range of applications.[1,5]

Nowadays, the global production of FPs uses polyols mainly derived from petrochemical raw materials. Consequently, the replacement of these components by more ecofriendly materials is a challenge that should be overcome not only because of uncertainty about the cost and availability of petroleum in the future but also because of human desires to obtain environmental advantages that originate in the use of renewable resources.[4,6]

The substitution of petrochemically derived feedstocks for PU synthesis by agricultural oils has been an area of intense research and development for several decades.[6–10] Moreover, much of this work has been predicated on the assumption that agriculturally derived building blocks will be competent replacements from both performance and economic standpoints. In this sense, the chemical modification of vegetable oils is a promising alternative in the production of green polyols,[4,8–11] which are mainly used for obtaining PU elastomers,[12,13] because the preparation of foams places an additional layer of complexity on data interpretation.[5,13]

Free-rise PU foams are generally obtained from the simultaneous reaction of a polyisocyanate with a polyol and water, where the latter is used as a reactive blowing agent. The reaction of the polyol with isocyanate produces urethane bonds; meanwhile, the reaction of the isocyanate with water generates urea and carbon dioxide. The gases generated inside drive the foam growth by expanding the gas bubbles entrapped in the reactive mixture. The polymer structure must build up rapidly to form a stable cellular structure but not so fast that it stops bubble growth. These two competing reactions are balanced by the addition of catalysts and surfactants.[9,13] Thus, the physical properties of foams must then not only be interpreted on the basis of the equilibrium structure but also on the effects of the competitive reactions involved.[13–15]

Several synthesis methods can be used to transform vegetable oils into polyols; these methods include ozonolysis, direct

oxidation, epoxidation followed by ring opening, and direct hydroxylation or transesterification with posterior functionalization of the fatty esters.[16–18] Herein, we studied the chemical modification of tung oil (TO), a nonedible oil, also called *China wood oil*, which is commonly used in wood finishing applications because of its drying properties. These properties are associated to its composition because of its high content of unsaturated fatty acids. In particular, α-eleostearic acid, a fatty acid with three conjugated double bonds, accounts for around 80% of the TO triglyceride composition. Multifunctional polyols can be obtained through the chemical modification of this oil, which can be further used as building blocks in biobased PU synthesis.

In this study, hydroxylated methyl esters (HMETO) and glycerol (GLY) were obtained with a two-step procedure as the main product and byproduct, respectively, of the chemical modification of TO. First, the fatty acid methyl esters from tung oil (METO) and GLY were obtained by means of alkaline transesterification. Then, the resulting METO was modified by hydroxylation with performic acid generated *in situ;* this resulted in HMETO. Both polyols (HMETO and GLY) were incorporated separately into a foam formulation based on a petrochemical polyether polyol, as crosslinker modifiers of relatively low molecular weight and functionality. Water was chosen as a chemical blowing agent, and a multifunctional prepolymer based on 4,4′-diphenylmethane diisocyanate (pMDI) was used as the isocyanate component. The effects of the modifications in the foam formulations on the characteristic times for foaming, density, morphology, and thermal and dynamic-mechanical properties of the FPs are presented and discussed.

EXPERIMENTAL

Materials

TO was provided by Cooperativa Agrícola Limitada de Picada Libertad. The chemicals used for the chemical modification of TO were absolute methanol (99.9%) and potassium hydroxide (KOH > 85%) from Biopack, hydrogen peroxide (30%) from Cicarelli, and formic acid (85.7% w/w) from Anedra. Sulfuric acid (98% w/w) and sodium bicarbonate (99%) from Anedra were used in the neutralization of the reaction products.

For the synthesis of the PU foams, pMDI (Rubinate 5005, Hunstman Polyurethanes) with an equivalent weight of 131 g/eq was used as the isocyanate component. The commercial polyether polyol (CPP) JEFFOL G31-35 (Hunstman Polyurethanes), with a low functionality (3.0), a relatively high molecular weight (4800 g/mol), a hydroxyl value of 35 mg of KOH/g, and an equivalent weight of 1600 g/eq, was selected to prepare the control flexible foams. Variable amounts of HMETO and GLY were used as "green" polyol components as partial replacements of the CPP. Distilled water was used as a unique and ecofriendly blowing agent, and other additives were added to the preparation: a surfactant agent (Tergostab B8404, Hunstman Polyurethanes), a tertiary amine as a blowing control catalyst (*N,N*-dimethylbenzyl amine, 99.9 wt %, Sigma-Aldrich), and a gelling control catalyst (dibutyltin dilaurate, 99.9 wt %, Sigma-Aldrich).

Methods

Preparation of Polyols from TO. ***Transesterification of TO (METO).*** The transesterification of TO was performed in a glass vessel provided with a mechanical mixer. A thermostatic oil bath was used to control the temperature. The procedure was carried out as follows: 300 mL of TO were preheated at 50 °C during 20 min and then, 1.8 g of KOH (previously dissolved in 90 mL of methanol) were poured into the vessel. The agitation and temperature were maintained at 350 rpm and 50 °C during the following 60 min. Afterwards, the mixture was allowed to settle during 2 h. Then, the upper layer containing the methyl esters was carefully transferred to a separating funnel and washed with a 0.015 N sulfuric acid solution and next with distilled water, until reaching neutral pH. Subsequently, the methyl esters were dried during 2 h at 70 °C with a BUCHI R-114 rotating evaporator equipped with a DOSIVAC vacuum pump. The pump operates at a pressure of 0.015 mmHg and with a flow rate of 5–7 mm^3/h.

Hydroxylation of methyl esters (HMETO). The hydroxylation of METO was performed with a molar ratio of 1:1.4:1 of double bonds to formic acid to hydrogen peroxide. Hydrogen peroxide (30% w/v) and formic acid (85 wt %) were mixed for 10 min in a stirred glass vessel at 25 °C. A thermostatic water bath was used to control the temperature. Then, the methyl esters were added dropwise for 2 h to prevent overheating, and the temperature was kept at 50 °C for 3 h. Once the reaction was finished, the reactor was cooled down to room temperature. The mixture was allowed to settle for 1 h into a separating funnel, and then, the bottom aqueous layer was removed. The product was neutralized with a 7% w/v $NaHCO_3$ solution and washed with distilled water up to a neutral pH. The upper layer was recovered and distilled *in vacuo* to remove water for 2 h at 70 °C with the rotating evaporator mentioned previously.

Preparation of FPs. The index (equivalents of NCO/equivalents of OH) was set at 1.1; the equivalents of OH provided by polyols and water were taken into account in this calculation. All of the formulations were based on the same total mass of the components. In all cases, 4 wt % water, 1.5 wt % surfactant, 3 wt % *N,N*-dimethylbenzyl amine, and 1.5 wt % dibutyltin dilaurate with respect to the total polyol mass were added. The polyols were dehydrated *in vacuo* at 70 °C before use. Different foams with their replicates were prepared: a reference foam based on Jeffol G31-35, modified foams with 5 and 10 wt % of GLY (5GLY and 10GLY, respectively), modified foams with 5 and 10 wt % of HMETO (5HMETO and 10HMETO, respectively), and a last sample modified with 10 wt % of GLY + 10 wt % of HMETO (10GLY10HMETO) with respect to the CPP mass in all cases. The foams were prepared by a free-rise procedure. Polyols, water, catalysts, and surfactant were weighed previously and mechanically mixed for 20 s. Then, pMDI was added, and the whole system was mixed for another 20 s. Characteristic times were recorded during the foam rising. The foams were stored for a week at room temperature before they were characterized.

Characterization Techniques. ***Hydroxyl number.*** The hydroxyl value of HMETO was determined according to ASTM D 4274, a procedure that is based on the acetylation of the sample with acetic anhydride in a pyridine solution.

Table I. Analytical Characterization of TO and its Derivatives

	TO	METO	HMETO
Hydroxyl value (mg of KOH/g)	0	0	163.2
Acid number (mg of KOH/g)	2.6	1.7	21.7
Saponification value (mg of KOH/g)	187.4	191.1	209.4
Iodine value (g of I/100 g)	182.2	161.2	31.6

Iodine value. The TO, METO, and HMETO iodine values were determined according to ASTM D 5554.

Fourier transform infrared (FTIR) spectroscopy. The FTIR spectra were recorded in a Genesis II FTIR spectrometer in transmission mode with NaCl plates. The spectra were recorded at a 2 cm^{-1} resolution, and the reported results are the average of 32 scans.

Density measurements. The density of the foams was calculated as the ratio between the weight and volume of a cylindrical specimen (28 mm in diameter × 30 mm in height). The weight was measured with a precision of 0.001 g and sample linear dimensions with an accuracy of 0.01 mm. The obtained values were averaged among four samples.

Scanning electron microscopy (SEM). The surfaces of the foams were analyzed with a JEOL JSM-6460 LV scanning electron microscope. Small specimens were cut from the middle of the foams in the direction of growth. The pieces were coated with gold before they were observed under the microscope.

Thermogravimetric analysis (TGA). The thermal decomposition curves were obtained with a Shimadzu TGA-50 thermogravimetric analyzer at a heating rate of 10 °C/min from 25 up to 800 °C under a nitrogen atmosphere.

Differential scanning calorimetry (DSC). These tests were performed with a TA Instruments DSQ-2000 differential scanning calorimeter with Tzero technology from D'Amico Systems at a heating rate of 20 °C/min under nitrogen atmosphere. The glass-transition temperature (T_g) values were determined at the midpoint of the observed change in the heat flux curve.

Dynamic mechanical analysis (DMA) tests. The dynamic mechanical properties of the samples were determined with an Anton Paar Physica MCR rheometer. Torsion geometry was used with cylindrical specimens 5 mm in thickness and 28 mm in diameter. Measurements were performed as temperature sweeps in the range −75 to 0 °C at a heating rate of 20 °C/min. The frequency was kept at 1 Hz, and the applied deformation was kept at 0.1% to ensure working in the linear viscoelastic range. The T_g values were arbitrarily taken as the temperature at which a maximum in the tan δ curve was observed.

RESULTS

Characterization of TO, METO, and HMETO

Table I presents the analytical characterization of TO and its derivatives. We noticed that as expected, the unmodified TO and METO had no OH groups and almost negligible amounts of free acids. After the hydroxylation reaction, the HMETO presented a hydroxyl number of 163.2 mg of KOH/g, and its acid value was higher than that of METO. This result indicates that not only hydroxyl groups (—OH) were added to the METO carbon chain but also that the formation of a small amount of free fatty acids took place during the hydroxylation reaction.

The iodine value of TO (182.2 g of I/100 g) showed a small decrease (161.2 g of I/100 g) after the transesterification reaction; this indicates that mostly all of the carbon–carbon unsaturations were preserved during this step of chemical modification. On the other hand, the iodine value of HMETO was significantly lower in comparison with that of the METO because the C═C bonds were reacted to introduce hydroxyl groups. Nevertheless, an iodine value higher than zero indicated that not all of the C═C bonds were reacted during the hydroxylation step.

The saponification (which jointly measures acid and ester groups) and acid values could be used to estimate the average molecular weight of TO and METO. Because TO has three ester groups and METO has just one, the results indicate that TO has an average molecular weight of 910.7 g/mol (1.098×10^{-3} mol/g), whereas that of METO was 296.2 g/mol (3.37×10^{-3} mol/g).

Figure 1 shows the FTIR spectra of TO, METO, and HMETO. As reported in a previous work,[19] the peaks at 3010 cm^{-1} (corresponding to the absorption of the C═C bonds) and 991 cm^{-1} (due to the absorption of the conjugated unsaturation of the α-eleostearic acid chains) were present in TO and remained in METO. This fact also confirmed that the C═C double bonds were conserved during the transesterification reaction. The intensities of the peaks at 1459 and 1430 cm^{-1} due to the asymmetric and symmetric vibrations of the C—H bonds of the methyl ester group (—$COOCH_3$) increased after transesterification; this confirmed that the reaction took place.

The main differences observed between the METO and HMETO spectra were the broad and more intense band of hydroxyl groups at 3500 cm^{-1} and the decrease in the stretching bands at

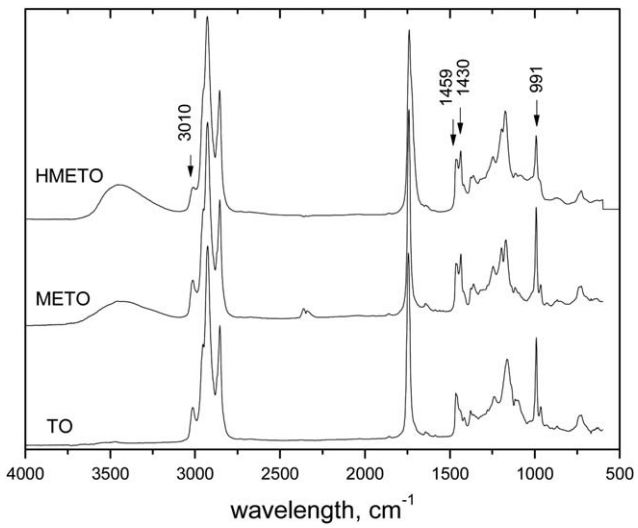

Figure 1. FTIR spectra of TO, METO, and HMETO.

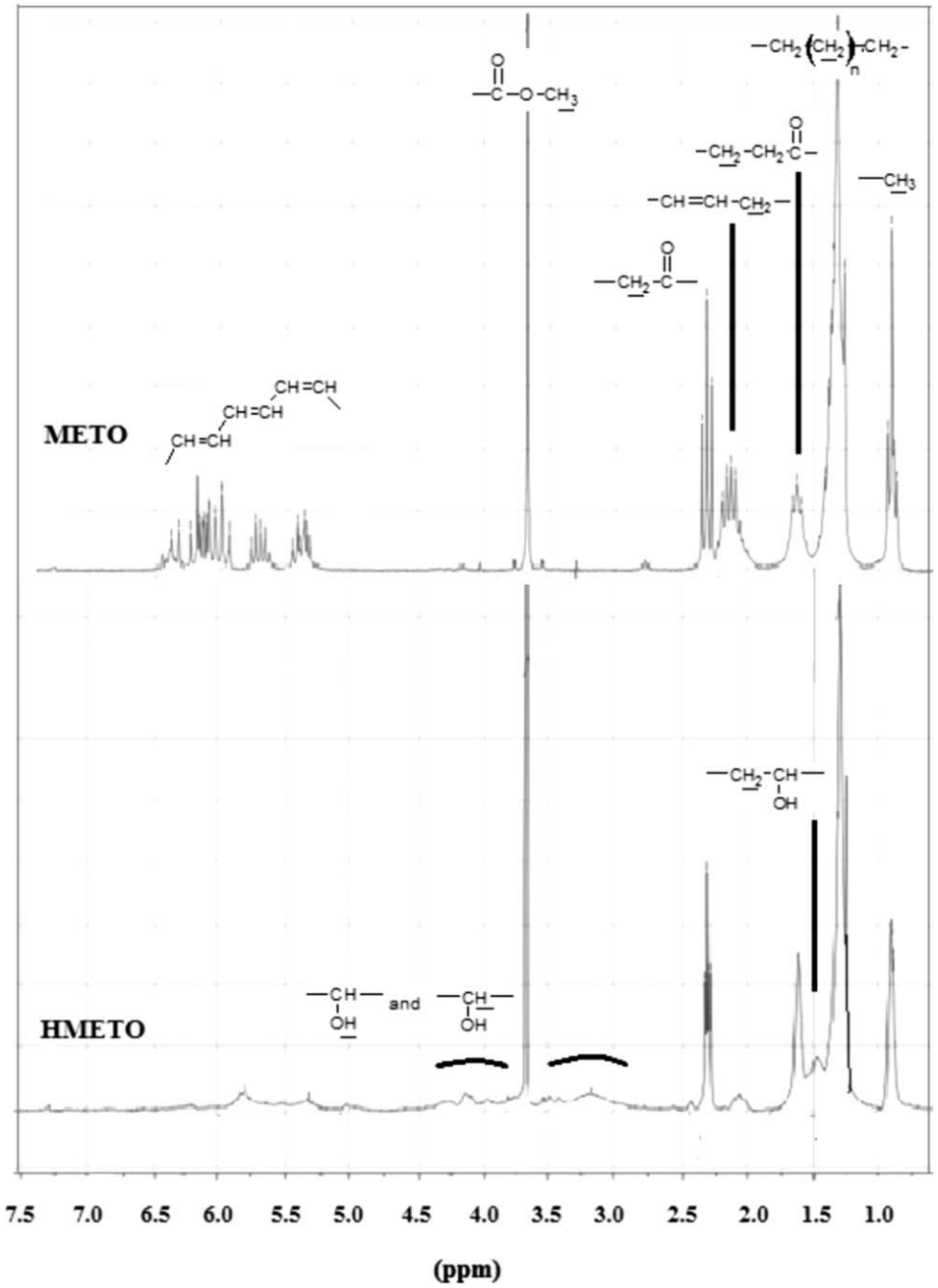

Figure 2. ^{1}H-NMR of METO and HMETO.

3010 and 991 cm^{-1} due to the attachment of hydroxyl groups to the C═C bonds after the hydroxylation reaction. These results agree with the reduction of the iodine value and the corresponding increased hydroxyl value in HMETO.

Figure 2 shows the ^{1}H-NMR spectra of METO and HMETO. The TO spectrum was analyzed in a previous work,[18] in which the main peaks were assigned as follows: 0.9 ppm, methyl protons at the end of the fatty acid chains; 1.3–1.4 olefinic protons separated by at least one carbon from the unsaturations; 1.6 ppm, olefinic protons separated by at least one carbon from the ester groups; 2.1 ppm, protons in the methylene groups close to the carbon–carbon unsaturations; 2.3–2.4 ppm (multiplets), methylene neighbor to the carboxylic groups in the triglycerides; 4.2–4.3 ppm, protons in the methylene groups and central proton of the GLY fragment; and 5.3–6.5 ppm, vinylic protons. The most important differences found in the METO spectrum (Figure 2) with respect to that of TO were (1) the almost negligible contribution of the peaks associated with the GLY structure (4.2–4.3 ppm) and (2) the new peak appearing at 3.7 ppm, which corresponds to the protons of the methyl group.[19] Moreover and as was already indicated, the double bonds were preserved during the transesterification reaction, which in the spectrum was denoted by the presence of the multiplets at 5.3–6.5 ppm. The differences between the METO and

Table II. Characteristic Times during the Preparation of the Foams

Sample	Cream time (s)	String time (s)	Rise time (s)	Tack-free time (min)
Reference foam	8.8 ± 1.1	22.6 ± 2.4	46.5 ± 6.3	1.12 ± 0.24
5GLY	8.1 ± 0.2	14.7 ± 0.1	22.0 ± 4.3	0.70 ± 0.07
10GLY	8.6 ± 1.2	14.7 ± 1.7	22.9 ± 2.1	0.56 ± 0.09
5HMETO	6.0 ± 2.8	23.5 ± 0.7	50.5 ± 2.1	1.12 ± 0.14
10HMETO	10.5 ± 0.7	27.5 ± 0.7	47.0 ± 1.4	1.22 ± 0.21
10GLY10HMETO	8.8 ± 0.5	15.9 ± 0.5	25.1 ± 2.0	0.62 ± 0.47

HMETO structures were also clear (Figure 2). HMETO exhibited reduced intensities of the multiplets at 5.2–6.5 ppm after the hydroxylation reaction; this indicated the important decrease in the amount of carbon–carbon double bonds. Furthermore, there was an increase in the area around the peak centered at 1.5 ppm; this was due to proton neighbors to the —CH—OH groups in HMETO.[20] This peak overlapped the peak corresponding to the olefinic protons separated by at least one carbon coming from the ester groups originally present in the METO. Moreover, the changes observed in the region of 3.0–4.5 ppm were also reported as chemical shifts for protons in carbons linked to hydroxyl groups.[11,21]

Characterization of the Foams

Modified foams were prepared by partial replacement of the petrochemical polyether polyol with HMETO and GLY separately incorporated (5 and 10 wt % with respect to the commercial polyol) or added together (10 wt % GLY + 10 wt % HMETO). The foams prepared with the formulations presented in this article did not collapse after curing, showing a stable and permanent cell structure. On the other hand, the attempts to replace more than 10% of the commercial polyol with one of the natural polyols or more than 20% with both were unsuccessful and led to the spontaneous collapse of the foam in about 1 day.

Cream, End of Rise, and Tack-Free Times. In the production of FPs two main reactions take place: the blow and gelation reactions.[8,10] Although these reactions proceeded in the absence of catalysts, the reaction rates are too slow.[10] Nevertheless, a correct balance is needed between both reaction rates. Indeed, if the blowing reaction proceeds relatively quickly, the cells may open before the polymer has enough strength to maintain the cellular structure, and thus, the foam may collapse.[8,10] On the other hand, if the gelation reaction overtakes the blowing reaction, this might lead to closed-cell foams[8] or just foam shrinkage.[10] The kinetically fastest reaction, between water and isocyanate, quickly forms polyurea segments and releases carbon dioxide gas; this expands the mixture. The hydroxyl isocyanate reaction gradually polymerizes isocyanates and polyols and builds up molecular weight. At a critical conversion, the entire system crosses the thermodynamic boundary of a miscible system, and phase separation occurs.[4,8,9] The resulting polymer is a segmented block copolymer with domains that are rich in either polyurea segments or polyol segments.[8,22] Within a domain rich in polyurea or PU, further association of the segments can also occur through hydrogen bonding.[8,23] Thus, a common method to determine the reaction rate of PU foam formation is to monitor the cream, gel (string), rise, and tack-free times.[8,24] The *cream time* is defined as the time taken for the reaction mixture to change from a clear color to a creamy color, the *gel time* is the time needed for an infinite network to be formed, the *rise time* is the time needed for the foam to fully expand,[8] and the *tack-free time* is the time at which the foam surface is no longer sticky at room temperature.

Table II shows the cream, string, rise, and tack-free times recorded during foam rising. The cream times of the foams modified with different contents of GLY were similar to that of the control foam. However, the string, tack-free, and end of rise times showed an important decrease with the addition of GLY to the formulation; this was associated with a quickening of the polymerization reaction that led to differences in the rate of viscosity rise during the foaming process[3] because of the higher reactivity of the hydroxyl groups in GLY (in comparison with that of CPP). GLY is a relatively small molecule with primary OH groups, whereas the polyol Jeffol G31-35 presented a much higher molecular and equivalent weights (4800 and 1600 g/eq, respectively).

On the other hand, the addition of HMETO did not significantly change the characteristic times of the reference foam, although HMETO also presented a lower equivalent weight (316.4 g/equiv) than the commercial polyol.

The characteristic times of the foam prepared with both modifiers (10 wt % GLY + 10 wt % HMETO) were intermediate between the corresponding times of the samples modified with 10 wt % HMETO and 10 wt % GLY, although they were closer to the latter because the facts discussed previously.

Generally, the surfactants were added to the PU foam formulation to stabilize bubble formation; this helped to control the cell size and cell opening and, by this means, enhance the operating margin between the extremes of collapse and shrinkage of the foam due to a high closed-cell content.[2] Moreover, most of the reactions occurring during the foaming process were catalyzed to allow extremely short reaction times. However, in this study, it was not possible to find an adequate formulation of modified FPs with percentages of GLY or HMETO higher than 10 wt %, even when the relative amounts of surfactants and catalysts were varied. Evidently, the lower reactivity of the commercial polyol associated with its higher equivalent weight tended to favor foam stability.

FTIR Analysis. Figure 3 shows the spectra of CPP, the reference foam (with only CPP as the polyol component), and PU foams

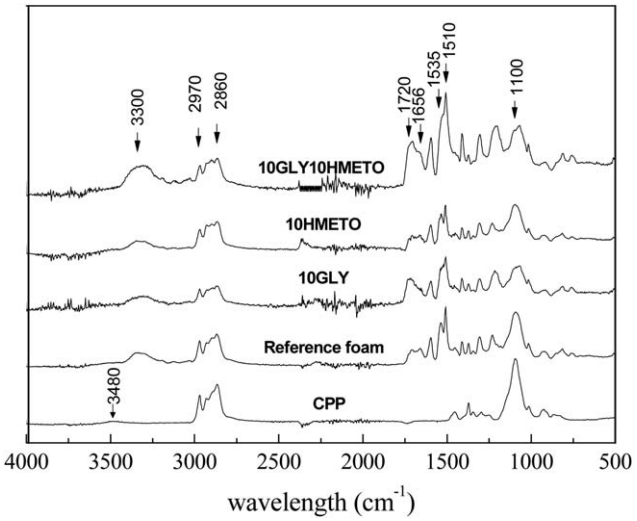

Figure 3. FTIR spectra of the CPP, reference foam, and modified foams with 10 wt % GLY, 10 wt % HMETO, and 10 wt % GLY plus 10 wt % HMETO.

modified with 10 wt % GLY, 10 wt % HMETO, and 10 wt % GLY plus 10 wt % HMETO. The CPP is a polyether polyol, and thus, its FTIR spectrum revealed the existence of stretching bands at 3480 cm^{-1} (O—H group) and 2970 and 2860 cm^{-1} (C—H and O—CH_2 groups) and one antisymmetric stretching band at 1100 cm^{-1} (C—O—C group). The reference PU presented signals corresponding to the stretching vibration of NH groups at 3300 cm^{-1}; this indicated the formation of urethane linkages. The wide band in the range 1640–1740 cm^{-1} was characteristic of the urea and urethane carbonyl (C═O) stretching vibrations, and the strong band at 1510 cm^{-1} corresponded to N—H deformation. At 1535 cm^{-1}, the amide-II band related to the stretching vibrations of C—N combined with the bending vibrations of N—H was also observed. Moreover, the band associated with the ether group of CPP (1100 cm^{-1}) was clearly noticed in the cured PU.

The most important changes in the FTIR spectra of the cured PUs were observed with the addition of GLY to the formulation. Because the CPP concentration decreased as GLY was added, the band corresponding to C—O—C (1100 cm^{-1}) and the bands at 2970 and 2860 cm^{-1} decreased their intensity. On the other hand, the addition of HMETO resulted in an increase in the bands between 2800 and 3000 cm^{-1} because of the increase in CH and CH_2 groups introduced by the fatty acid fragments of HMETO. Moreover, the band in the region 1640–1740 cm^{-1}, which provided valuable information on hydrogen bonding and the ordering of hard segments,[25,26] can be further analyzed. This wide band could be split in two peaks, one at about 1720 cm^{-1} coming from the non-hydrogen-bonded urethane carbonyl and other corresponding to the carbonyl absorption at about 1656 cm^{-1} (amide I). This last peak could also be assigned to the overlap of two peaks corresponding to tridimensional ordered urea segments or bidentate hydrogen-bonded urea (1643 cm^{-1})[4,25] and to shorter, nonordered, or monodentate hydrogen-bonded urea segments (1673 cm^{-1}).[25] In this sense, we noticed that in the reference foam and the foam with HMETO, both contributions were of about the same intensity, whereas the urea contribution was significantly lower in the foam modified with GLY. The different ratios between the absorption intensity of these two signals were indicative of phase separation within the material,[8,9,27] being the hydrogen-bonded urea, including both monodentate and bidentate an indication of hard domains inside the foam structure.[9]

The spectrum of the foam made from both natural polyols was similar to that of the 10GLY foam, with regard the 1640–1740 cm^{-1} zone. However, no decrease in the intensity of the bands at 2970 and 2860 cm^{-1} with respect to those of the reference foam was observed; this was probably due to the contribution of the HMETO (higher equivalent weight than GLY). Moreover, the wide band at 3300 cm^{-1} and the peak at 1510 cm^{-1} (N—H vibration and deformation, respectively) were larger than those corresponding to the other samples; this indicated an increased concentration of urethane linkages.

The presence of a very small signal at 2260 cm^{-1} (N═C═O) denoted that small amounts of unreacted isocyanate remained in all of the cured foams.[8] However, a 10% excess of isocyanate was deliberately used in the PU preparation to ensure complete conversion of polyols to urethanes due to the occurrence of the unavoidable isocyanate-consuming side reactions.

Densities and Morphologies. Table III presents the densities of the different foams. The average density of the reference foam was 31.9 kg/m^3, and it increased with increasing GLY content. This was associated with the higher reactivity of the GLY, which increased the reaction rate. Consequently, the foam reached the gel point and the end rise before reaching the same height of the reference one. Moreover, in a previous work, it was demonstrated that the addition of GLY increased the density of the PU network because of the decrease in chain length between crosslinking points.[28] Thus, these higher density values could be related not only to the increased crosslinking density but also to a lower volume expansion of foams. The addition of HMETO also increased, to some extent, the density of the foam; this could also be related to the higher functionality (per gram of sample) of the TO derivative in comparison with that of the synthetic polyol, although it was lower than that of GLY. The foam prepared with both GLY and HMETO presented an intermediate density between that of the 10% HMETO and 10% GLY foams because both effects contributed to the development of its structure.

Table III. Densities of the Foams

Sample	Density (Kg/m^3)
Reference foam	31.9 ± 2.3
5GLY	52.1 ± 1.8
10GLY	65.4 ± 3.0
5HMETO	32.2 ± 2.6
10HMETO	36.6 ± 4.7
10GLY10HMETO	62.8 ± 10.3

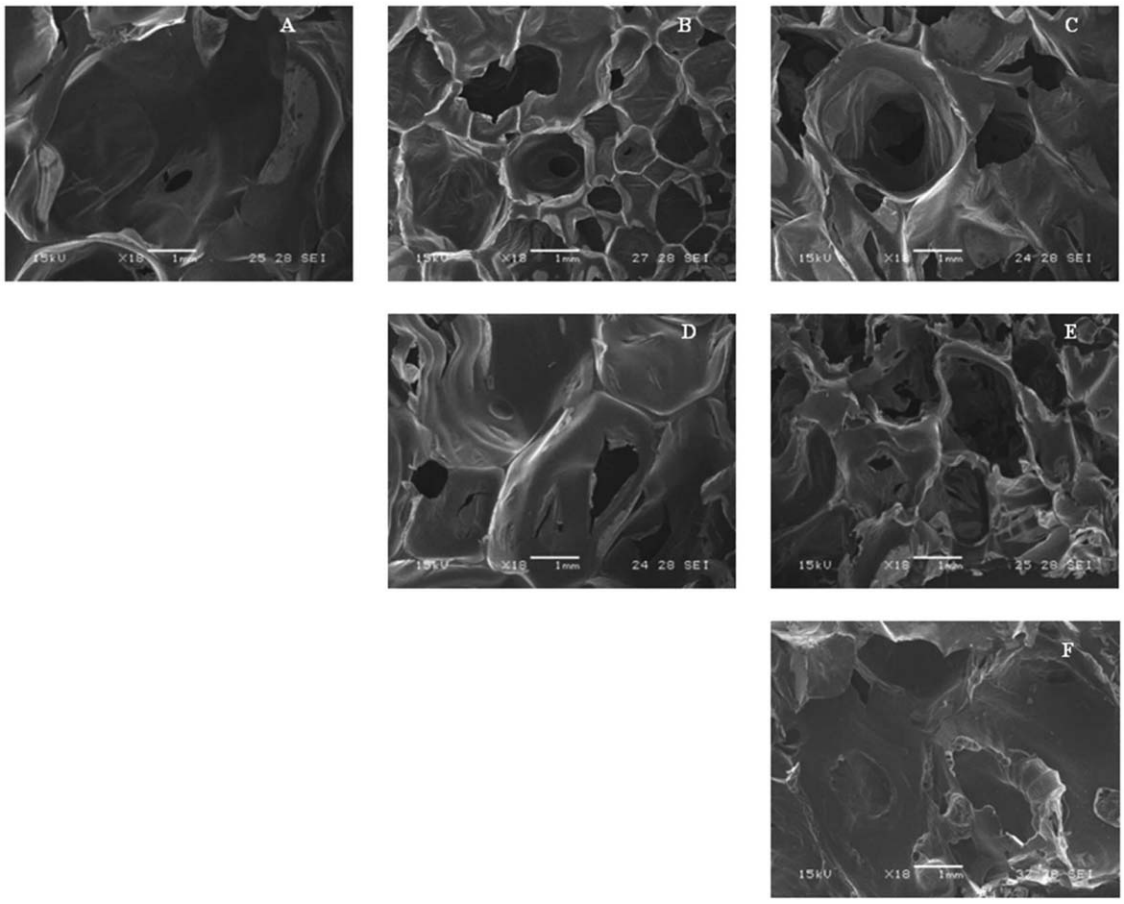

Figure 4. SEM micrographs of selected foams: (A) reference foam, (B) 5HMETO, (C) 10HMETO, (D) 5GLY, (E) 10GLY, and (F) 10GLY10HMETO.

Figure 4 shows SEM micrographs of samples cut from the middle of the foams in the direction of growth. All of the foams presented a mix between a closed and open cellular structure with small pores and a greater tendency for incomplete cell opening in the control foam, as compared with the modified ones.[3] Other authors reported that even when flexible foams were designed to be an open-celled structure, they also presented, at least, a small number of closed cells, as confirmed by SEM observations.[8]

In all cases, we observed preferential orientation associated with the foam rise direction. Meanwhile, the cellular structure perpendicular to the foaming direction appeared isotropic in all cases (images not shown). The partial replacement of the synthetic polyol with GLY or HMETO led to smaller cells with a narrow distribution of sizes in agreement with the higher densities of the foams. In general, decreased cell sizes can be favored by decreased gas diffusion,[1] which in turn could be associated with the limited expansion of the modified foams.

The foam based on HMETO had a cellular structure with a mostly equiaxed polygonal shape, with average diameters ranging from 0.5 to 2 mm, whereas the foams modified with GLY present a more distorted structure, with irregularly shaped cells. As discussed previously, the more reactive GLY (in comparison with CPP) built viscosity faster and gel earlier. Thus, it allowed a relatively small time for the setting up of regular and uniform cells. The associated increase in viscosity tended to arrest bubble growth earlier and produced foams with smaller cells and a decreased tendency to expand as the GLY content increased. On the other hand, when the commercial polyol was partially replaced by HMETO, there was little propensity for the incorporation of crosslinks into urea-based domains (this was due to the lower reactivity of HMETO as compared with GLY), and the increase in viscosity occurred more slowly. This led to more regular cells than those obtained in the foams modified with GLY.

The foam prepared with both natural polyols presented an even more distorted cell structure than those based on GLY with regard to the form and also to the size distribution. We also observed a larger content of closed cells; this resulted from the combination of factors discussed previously, with those related to the GLY contribution prevailing, as inferred from the relatively low characteristic times exhibited during polymerization. Similar results were also found by Lan *et al.*[3]

Thermogravimetric Analysis (TGA). Thermogravimetric tests were performed to study the thermal decomposition behavior of the obtained PU foams and to evaluate the effects of addition of GLY and HMETO. Thermograms of selected foams are shown in Figure 5. Similar thermal behavior was observed among the petrochemical-based control foam and the modified foams with

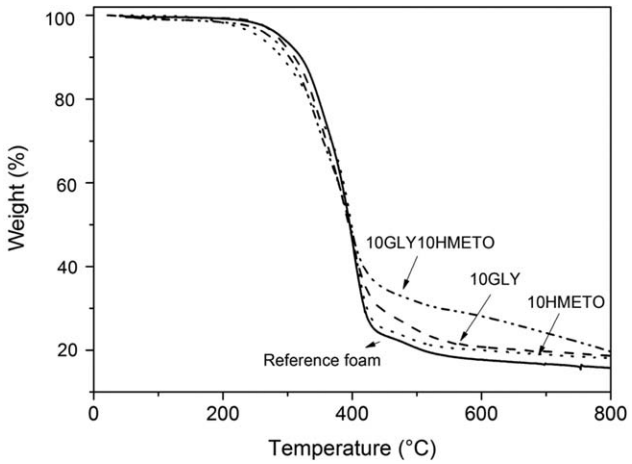

Figure 5. TGA curves of selected foams: reference foam, 10HMETO, 10GLY, and 10GLY10HMETO.

biobased polyols. All samples showed two-step thermal degradation patterns with maximum degradation rates occurring at 335–350 °C (first step, with the lower values corresponding to the HMETO-modified foams) and 390–400 °C (second step).

The first peak, which involved a total weight loss of around 15–20%, was related to the dissociation of urethane bonds; it took place either through the dissociation into isocyanate and alcohol or the formation of the primary or secondary amines olefin and carbon dioxide.[29–31] The second degradation step was associated with the decomposition of the soft segment (polyol backbone) into carbon monoxide, carbon dioxide, carbonyls (aldehyde, acid, acrolein), olefins, and alkenes.[30–32] This step involved the largest weight loss, approximately 47–53% of the total. The loss of weight at temperatures higher than 400 °C corresponded to the decomposition of fragments such as esters or more strongly bonded fragments associated with the polyol backbone that occurs at high temperature and probably to the degradation of the remaining carbonaceous materials from the previous steps.[31,33]

Table IV reports the onset temperature and the char residue values obtained at 600 °C. The onset of decomposition, defined as the temperature at which the weight loss reaches 5 wt %, appeared at lower temperatures for the modified foams. The largest difference was obtained among the foams modified with HMETO and the reference foam, which exhibited mean (average values for 5 and 10% HMETO) onset temperature values close to 255 and 290 °C, respectively. On the other hand, the foams modified with GLY showed only a slight difference with respect to the reference foam because their average onset temperature was about 280 °C. As discussed previously, after the chemical modifications of TO and METO to finally obtain HMETO, we found that a small fraction of fatty acids was not able to introduce reactive hydroxyl groups, and thus, some C—C double bonds remained unreacted during the hydroxylation reaction (nonzero iodine value). These fatty acids or fragments of them (dangling chains) started their thermal degradation at lower temperatures than the higher crosslinked main structure of the PU. This behavior was also noticed in related works: Bernardini *et al.*[9] reported that the presence of double bonds in the castor oil molecules (polyol) made their foam structure weaker with respect to thermal degradation. As expected, the foam based in both natural polyols presented an intermediate thermal degradation behavior between that of the 10 wt % HMETO and 10 wt % GLY up to 400 °C (including the onset temperature value). At 600 °C, the modified foams presented a slightly higher residual mass than the control foam (ca. 16% for 10HMETO and 24% for 10GLY), which can be related to a better behavior under fire. Nevertheless, the char residue of the foam prepared with both biopolyols was the largest among the specimens tested because of the increased contribution of biobased polyols (20% of the total polyol content).

Even though the onset temperature was lower for the modified foams as compared to the control foam, the formation of char layers would considerably slow down the thermal decomposition.[34] According to Bernardini *et al.*,[9] a higher amount of carbon residues can be associated with a more regular cellular structure, which would hinder the regular heat transfer and, therefore, would result in a less efficient pyrolysis. However, this reasoning did not explain what was observed in this study because the PU–GLY foams presented the most irregular foam structures, and thus, this behavior was mainly associated to the higher density of these foams. The overall thermal stability of these biopolyol-based foams was good and compared fairly well with commercial foams and other vegetable-based polyol foams.[31,35,36]

Thermal and Dynamic-Mechanical Characterization. Figure 6 shows the curves of heat flow versus temperature obtained from DSC measurements. Although these curves indicated very wide

Table IV. TGA Results

Sample	Onset temperature (°C)	Char residue (g/g)	Temperature for maximum degradation rate (°C)	
			First step	Second step
Reference foam	289.5	0.1774	352	402
5HMETO	254.6	0.2118	339	398
10HMETO	256.0	0.2003	336	402
5GLY	276.7	0.2319	346	390
10GLY	283.9	0.2078	347	399
10GLY10HMETO	272.5	0.2814	343	396

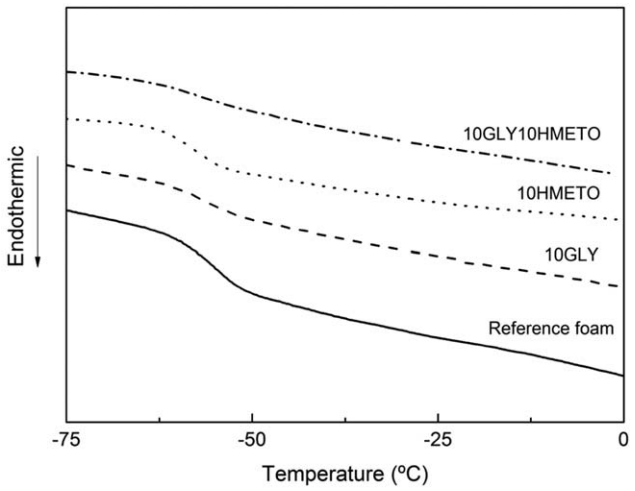

Figure 6. DSC curves for the reference foam and foams modified with 10 wt % GLY, 10 wt % HMETO, and 10 wt % GLY plus 10 wt % HMETO.

thermal transitions, as happens in heterogeneous crosslinked thermosets, it was possible to determine the T_g values of the samples as the midpoints of the change in the heat flux curve. As was expected for flexible foams, the main transition appeared at temperatures below room temperature for all of the samples. As a general tendency, the T_g values shifted slightly to lower temperatures as the commercial polyol was replaced by the natural ones, although the differences were not significant.

DMA is a precise technique that provides information about viscoelastic properties like stiffness and energy dissipation of soft and hard materials and thus, was selected to complement the characterization of the foams. Figures 7 and 8 show the dynamic mechanical properties of foams with different compositions. In particular, Figure 7 shows the experimental curves of tan δ versus temperature. The position of the maximum in the tan δ curve was taken as T_g of the samples. As it was aforementioned, the transitions are very broad, mainly in the foams containing 10 wt % GLY. This fact and the decrease in the height of the tan δ peak could be related to a more crosslinked and heterogeneous network, with decreased energy absorption capacity, as compared with the foams that do not contain GLY.

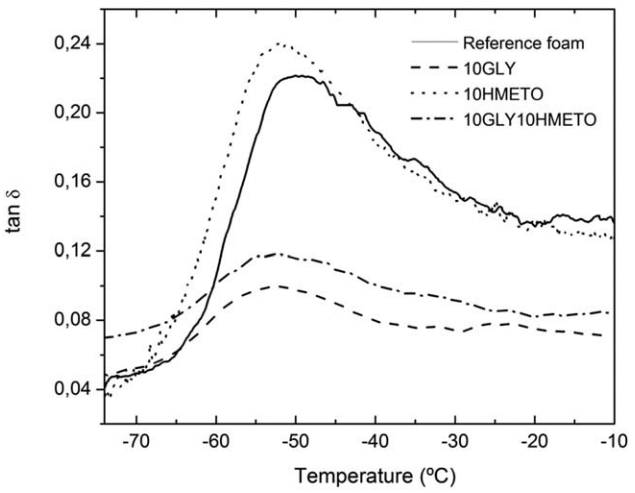

Figure 7. Tan δ versus temperature for the reference and modified foams with 10 wt % GLY, 10 wt % HMETO, and 10 wt % GLY plus 10 wt % HMETO.

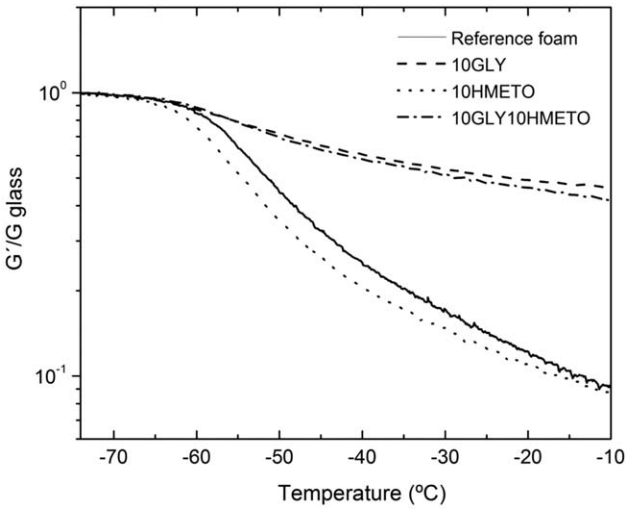

Figure 8. Relative shear storage modulus (G'/G' glassy modulus at −75 °C) versus the temperature for the reference and modified foams with 10 wt % GLY, 10 wt % HMETO, and 10 wt % GLY plus 10 wt % HMETO.

Table V summarizes the T_g values obtained by DSC and DMA. Although the DSC and DMA results show clear differences in the obtained values (because the T_g values were dependent on the conditions of the measurement and the method chosen for its determination), the trend was the same in both determinations.

The curves of relative shear storage modulus (G′; values divided by the glassy shear storage modulus of each sample at −75 °C) as a function of the temperature are presented in Figure 8. The porous nature of the foams made it very difficult to measure the real area and, hence, to obtain reliable modulus values.[4,37] Moreover, these foams, which were flexible at room temperature, could undergo significant shrinkage as the temperature decreased below T_g; this made it even more difficult to determine the area of the specimen under testing as the temperature changes and consequently affects the values of the storage modulus. To prevent these problems, the influence of the area in the measurements was eliminated by normalization of the storage modulus with the corresponding shear glassy moduli as reference values.

Table V. T_g Values Determined from DSC and DMA Measurements

	T_g (°C)	
Sample	DSC	DMA
Reference foam	−55.6	−49.6
10GLY	−56.9	−52.1
10HMETO	−58.5	−51.7
10GLY10HMETO	−57.5	−52.4

The storage modulus showed the typical drop from the region at low temperatures corresponding to the glassy state to the one at high temperatures corresponding to the rubbery state of the foams. In addition, as shown in Figure 8, the samples 10GLY and 10GLY10HMETO showed the widest transitions, whereas the reference foam and the sample 10HMETO presented the lowest moduli above T_g.

The rubber modulus was correlated with the crosslinking density of the material and with the rigidity of the crosslinking points, which increased as GLY was added to the foam formulation. Moreover, the storage modulus at temperatures above T_g was also directly related to the foam density (measured at room temperature), and thus, the highest values were observed for the 10GLY and 10GLY10HMETO foams. On the other hand, the relative decrease in dangling chains corresponding to the fatty acid chains (known to have a plasticizing effect because they are elastically ineffective[12]) when GLY was incorporated into the 10GLY10HMETO foam also contributed to the increase in the rubbery modulus of this foam.

CONCLUSIONS

HMETO and GLY as biobased polyols were successfully derived from TO according to a simple two-step method. Both natural polyols could be used to partially replace a petrochemical polyol in the formulation of FPs; this leds to more ecofriendly formulations with properties comparable to the reference one. Specifically, modified foams showed higher densities and a morphology with smaller cells than the reference foam; this was related to an increased crosslinking density of the PU network. The thermal degradation patterns of the modified foams were quite similar to that of the commercial formulation, although their char residues were somewhat larger because of the increased contribution of biobased polyols. GLY acted as a more effective crosslinker agent than HMETO, and this was reflected in the higher rubbery modulus of the foams modified with this biobased polyol.

ACKNOWLEDGMENTS

The authors gratefully acknowledge the financial support provided by the National Research Council of Argentina (contract grant numbers PIP 0637 and 0866), the Science and Technology National Promotion Agency (contract grant number PICT-2013-1535), and the National University of Mar del Plata (contract grant number 15/G430).

REFERENCES

1. Verdejo, R.; Stämpfli, R.; Alvarez-Lainez, M.; Mourad, S.; Rodriguez-Perez, M. A.; Brühwiler, P. A.; Shaffer, M. *Compos. Sci. Technol.* **2009**, *69*, 1564.
2. Lefebvre, J.; Bastin, B.; Le Bras, M.; Duquesne, S.; Paleja, R.; Delobel, R. *Polym. Degrad. Stab.* **2005**, *88*, 28.
3. Lan, Z.; Daga, R.; Whitehouse, R.; McCarthy, S.; Schmidt, D. *Polymer* **2014**, *55*, 2635.
4. Ugarte, L.; Saralegi, A.; Fernández, R.; Marín, L.; Corcuera, M. A.; Eceiza, A. *Ind. Crops Prod.* **2014**, *62*, 545.
5. Herrington, R.; Broos, R.; Knaub, P. In Handbook of Polymeric Foams and Foam Technology, 2nd ed.; Klempner, D., Sendijarevic, V., Eds.; Hanser: Cincinnati, **2004**; Chapter 4, p 55.
6. Sonnenschein, M. F.; Wendt, B. L. *Polymer* **2013**, *54*, 2511.
7. Petrovic, Z. S.; Fajnik, D. J. *Appl. Polym. Sci.* **1984**, *29*, 1031.
8. Cinelli, P.; Anguillesi, I.; Lazzeri, A. *Eur. Polym. J.* **2013**, *49*, 1174.
9. Bernardini, J.; Cinelli, P.; Anguillesi, I.; Coltelli, M. B.; Lazzeri, A. *Eur. Polym. J.* **2015**, *64*, 147.
10. Gama, N. V.; Soares, B.; Freire, C. S. R.; Silva, R.; Neto, C. P.; Barros-Timmons, A.; Ferreira, A. *Mater. Des.* **2015**, *76*, 77.
11. Caillol, S.; Desroches, M.; Boutevin, G.; Loubat, C.; Auvergne, R.; Boutevin, B. *Eur. J. Lipid Sci. Technol.* **2012**, *114*, 1447.
12. Ferrer, M. C. C.; Babb, D.; Ryan, A. *J. Polymer* **2008**, *49*, 3279.
13. Sonnenschein, M. F.; Ginzburg, V. V.; Schiller, K. S.; Wendt, B. L. *Polymer* **2013**, *54*, 1350.
14. Pannone, M. C.; Macosko, C. W. *J. Appl. Polym. Sci.* **1987**, *34*, 2409.
15. Hamley, I. W.; Stanford, J. L.; Wilkinson, A. N.; Elwell, M. J.; Ryan, A. J. *Polymer* **2000**, *41*, 2569.
16. Desroches, M.; Escouvois, M.; Auvergne, R.; Caillol, S.; Boutevin, B. *Polym. Rev.* **2012**, *52*, 38.
17. Khot, S. N.; Lascala, J. J.; Can, E.; Morye, S. S.; Williams, G. I.; Palmese, G. R.; Kusefoglu, S. H.; Wool, R. P. *J. Appl. Polym. Sci.* **2001**, *82*, 703.
18. Mosiewicki, M. A.; Casado, U.; Marcovich, N. E.; Aranguren, M. I. *Polym. Eng. Sci.* **2009**, *49*, 685.
19. Meiorin, C.; Aranguren, M. I.; Mosiewicki, M. A. *Eur. Polym. J.* **2015**, *67*, 551.
20. Tran, N. B.; Vialle, J.; Pham, Q. T. *Polymer* **1997**, *38*, 2467.
21. Zhang, J.; Zhao, Y.-J.; Su, Z.-G.; Ma, G.-H. *J. Appl. Polym. Sci.* **2007**, *105*, 3782.
22. Cooper, S. L.; Tobolsky, A. V. *J. Appl. Polym. Sci.* **1966**, *10*, 1837.
23. Coleman, M. M.; Lee, K. H.; Skrovanek, D. J.; Painter, P. C. *Macromolecules* **1986**, *19*, 2149.
24. Kim, Y. K.; Kim, C. U. *J. Ind. Eng. Chem.* **1997**, *3*, 138.
25. Javni, I.; Song, K.; Lin, J.; Petrovic, Z. S. *J. Cell Plast.* **2011**, *47*, 357.
26. Kwon, O. J.; Oh, S. T.; Lee, S. D.; Lee, N. R.; Shin, C. H.; Park, J. S. *Fiber Polym.* **2007**, *8*, 347.
27. Zhang, X. D.; Bertsch, L. M.; Makosco, C. W.; Turner, R. B.; House, D. W.; Scott, R. V. *Cell Polym.* **1998**, *17*, 327.
28. Calvo-Correas, T.; Mosiewicki, M. A.; Corcuera, M.; Eceiza, A.; Aranguren, M. I. J. *Renew. Mater.* **2015**, *3*, 3.
29. Javni, I.; Petrovic, Z. S.; Guo, A.; Fuller, R. *J. Appl. Polym. Sci.* **2000**, *77*, 1723.
30. Shufen, L.; Zhi, J.; Kaijun, Y.; Shuqin, Y.; Chow, W. *Polym. Plast. Technol.* **2006**, *45*, 95.
31. Pillai, P. K. S.; Li, S.; Bouzidi, L.; Narine, S. S. *Ind. Crops Prod.* **2016**, *83*, 568.

32. Gryglewicz, S.; Piechocki, W.; Gryglewicz, G. *Bioresour. Technol.* **2003**, *87*, 35.
33. Lin, B.; Yang, L.; Dai, H.; Hou, Q.; Zhang, L. *J. Therm. Anal. Calorim.* **2009**, *95*, 977.
34. Beyler, C. *Fire Saf. Sci.* **2005**, *8*, 1047.
35. Guo, A.; Javni, I.; Petrovic, Z. *J. Appl. Polym. Sci.* **2000**, *77*, 467.
36. Pawlik, H.; Prociak, A. *J. Polym. Environ.* **2012**, *20*, 438.
37. Das, S.; Dave, M.; Wilkes, G. L. *J. Appl. Polym. Sci.* **2009**, *112*, 299.